



Inverse Load Calculation of Wind Turbine Support Structures – A Numerical Verification Using the Comprehensive Simulation Code FAST

Preprint

Thomas Pahn and Raimund Rolfes
Leibniz Universität Hannover

Jason Jonkman and Amy Robertson
National Renewable Energy Laboratory

*Presented at the 53rd Structures, Structural Dynamics, and Materials Conference
Honolulu, Hawaii
April 23 – 26, 2012*

NREL is a national laboratory of the U.S. Department of Energy, Office of Energy Efficiency & Renewable Energy, operated by the Alliance for Sustainable Energy, LLC.

Conference Paper
NREL/CP-5000-54675
Revised November 2012

Contract No. DE-AC36-08GO28308

NOTICE

The submitted manuscript has been offered by an employee of the Alliance for Sustainable Energy, LLC (Alliance), a contractor of the US Government under Contract No. DE-AC36-08GO28308. Accordingly, the US Government and Alliance retain a nonexclusive royalty-free license to publish or reproduce the published form of this contribution, or allow others to do so, for US Government purposes.

This report was prepared as an account of work sponsored by an agency of the United States government. Neither the United States government nor any agency thereof, nor any of their employees, makes any warranty, express or implied, or assumes any legal liability or responsibility for the accuracy, completeness, or usefulness of any information, apparatus, product, or process disclosed, or represents that its use would not infringe privately owned rights. Reference herein to any specific commercial product, process, or service by trade name, trademark, manufacturer, or otherwise does not necessarily constitute or imply its endorsement, recommendation, or favoring by the United States government or any agency thereof. The views and opinions of authors expressed herein do not necessarily state or reflect those of the United States government or any agency thereof.

Available electronically at <http://www.osti.gov/bridge>

Available for a processing fee to U.S. Department of Energy and its contractors, in paper, from:

U.S. Department of Energy
Office of Scientific and Technical Information
P.O. Box 62
Oak Ridge, TN 37831-0062
phone: 865.576.8401
fax: 865.576.5728
email: <mailto:reports@adonis.osti.gov>

Available for sale to the public, in paper, from:

U.S. Department of Commerce
National Technical Information Service
5285 Port Royal Road
Springfield, VA 22161
phone: 800.553.6847
fax: 703.605.6900
email: orders@ntis.fedworld.gov
online ordering: <http://www.ntis.gov/help/ordermethods.aspx>

Cover Photos: (left to right) PIX 16416, PIX 17423, PIX 16560, PIX 17613, PIX 17436, PIX 17721



Printed on paper containing at least 50% wastepaper, including 10% post consumer waste.

ERRATA SHEET

NREL REPORT/PROJECT NUMBER:NREL/CP-5000-54675

TITLE: Inverse Load Calculation of Wind Turbine Support Structures - A Numerical

Verification Using the Comprehensive Simulation Code FAST: Preprint

AUTHORS: Thomas Pahn and Raimund Rolfes, Leibniz Universitat Hannover, and

Jason Jonkman and Amy Robertson, NREL

ORIGINAL PUBLICATION DATE: April 2012

DATE OF CORRECTIONS: November 2012

The following corrections were made to this report/document:

A previous version of this paper, available until November 28, 2012, incorrectly calculated the differences between the dynamic components of the inverse load and the rotor thrust in Figures 5, 8, and 11. These figures have been replaced and now illustrate the correct calculations.

Inverse load calculation of wind turbine support structures – a numerical verification using the comprehensive simulation code FAST

Thomas Pahn¹

Leibniz Universität Hannover (LUH), Hannover, Germany

Jason Jonkman²

National Renewable Energy Laboratory (NREL), Golden CO, United States of America

Raimund Rolfes³

Leibniz Universität Hannover (LUH), Hannover, Germany

Amy Robertson⁴

National Renewable Energy Laboratory (NREL), Golden CO, United States of America

Physically measuring the dynamic responses of wind turbine support structures enables the calculation of the applied loads using an inverse procedure. In this process, inverse means deriving the inputs/forces from the outputs/responses. This paper presents results of a numerical verification of such an inverse load calculation. For this verification, the comprehensive simulation code FAST is used. FAST accounts for the coupled dynamics of wind inflow, aerodynamics, elasticity and turbine controls. Simulations are run using a 5-MW onshore wind turbine model with a tubular tower. Both the applied loads due to the instantaneous wind field and the resulting system responses are known from the simulations. Using the system responses as inputs to the inverse calculation, the applied loads are calculated, which in this case are the rotor thrust forces. These forces are compared to the rotor thrust forces known from the FAST simulations. The results of these comparisons are presented to assess the accuracy of the inverse calculation. To study the influences of turbine controls, load cases in normal operation between cut-in and rated wind speed, near rated wind speed and between rated and cut-out wind speed are chosen. The presented study shows that the inverse load calculation is capable of computing very good estimates of the rotor thrust. The accuracy of the inverse calculation does not depend on the control activity of the wind turbine.

Nomenclature

\mathbf{B}_E	=	viscous modal damping matrix
\mathbf{D}	=	damping matrix
D_i	=	modal damping ratio
\mathbf{F}	=	Fourier transform of the force vector
F_{inv}	=	inversely calculated load
$\mathbf{f}(t)$	=	force vector
$f(t)$	=	force signal

¹ Dipl.-Ing., Institut für Statik und Dynamik (ISD), Appelstraße 9A 30167 Hannover.

² Ph.D., National Wind Technology Center (NWTC), 1617 Cole Blvd Golden CO 80410-3393, AIAA Professional Member.

³ Prof. Dr.-Ing. habil., Institut für Statik und Dynamik (ISD), Appelstraße 9A 30167 Hannover.

⁴ Ph.D., National Wind Technology Center (NWTC), 1617 Cole Blvd Golden CO 80410-3393.

f	= frequency
f_{0i}	= eigenfrequency in Hz
$\mathbf{H}(j\omega)$	= frequency response function (FRF) matrix
$\mathbf{H}_g(j\omega)$	= generalized FRF matrix
i	= number of vibration mode
\mathbf{M}	= mass matrix
\mathbf{M}_g^{red}	= generalized mass matrix of the reduced system
m_{gi}	= entry of the generalized mass matrix of the reduced system
\mathbf{K}	= stiffness matrix
\mathbf{K}_g^{red}	= generalized stiffness matrix of the reduced system
k	= stiffness
RotThrust	= rotor thrust from FAST simulation
t	= time
\mathbf{U}_0	= modal matrix
$\mathbf{Y}(j\omega)$	= Fourier transform of the displacement vector
$\mathbf{y}(t)$	= displacement vector
$y(t)$	= displacement signal
$\dot{\mathbf{y}}(t)$	= velocity vector
$\ddot{\mathbf{y}}(t)$	= acceleration vector
ω	= angular frequency
ω_{0i}	= eigenfrequency in s^{-1}

I. Introduction

Knowing the loads acting on wind turbine structures is essential for different reasons. First of all, load assumptions used for the structural design need to be verified, as stated by the International Electrotechnical Commission Technical Standard (IEC TS) 61400-13¹. Also, knowing the acting loads is important in terms of structural health monitoring, especially for offshore wind turbines. At least 10 % of all offshore wind turbines in German waters will be equipped with monitoring systems to ensure the reliability of the support structures. This requirement is demanded by a standard published for the BSH (Federal Maritime and Hydrographic Agency, Germany)². Finally, from the means of realistic load values, lifetime predictions can be calculated.

To determine the applied loads, inverse load calculation procedures can be used. To apply such a procedure, the structural-dynamic behavior of the wind turbine needs to be accurately modeled. Then, measured dynamic structural responses such as accelerations can be used to calculate the applied force values. This concept is not new and has been successfully used in various fields – for instance in aviation^{3,4}, automotive industry^{5,6}, dynamically operating machines⁷, and even in geophysical sciences⁸. Recently, these procedures have been applied to wind turbines. Ref. 9 and 10 describe laboratory tests of simple structures under stochastic loads. These tests were aimed mainly at verifying the numerical accuracy of the inverse calculation procedure and thus do not account for the coupled dynamics of the blades and structure, nor do they allow the inclusion of wind turbine control. In Ref. 11 and 12, the results of inverse load calculations of two operating 5-MW wind turbines are shown. However, although all authors present excellent results, a verification of the calculated forces is not possible due to the fact that real load values hardly can be measured.

Hence, an important intermediate step has not been investigated yet: what effects do these coupled dynamics and turbine control have in relation to the inverse load calculation? These aspects are investigated using the comprehensive simulation code FAST¹³. FAST accounts for these effects. Furthermore, aside from the calculated structural responses, the loads are known. This approach provides the basis for a discussion about the accuracy of inverse load calculation when applied to wind turbine structures.

II. Procedure of the inverse load calculation

Different numerical methods exist to calculate loads inversely. Generally, these methods can be divided into time-domain and frequency-domain approaches. Both have their advantages and drawbacks. Evaluative summaries are given in Ref. 6, 7 and 14. This paper seeks to verify the frequency-based procedures presented in Ref. 12 and 15. The fundamental theoretical principles of this approach are described briefly below.

The equation of motion for a discrete linear dynamical system can be described by the following second order ordinary differential equation in the time domain.

$$\mathbf{M}\ddot{\mathbf{y}}(t) + \mathbf{D}\dot{\mathbf{y}}(t) + \mathbf{K}\mathbf{y}(t) = \mathbf{f}(t) \quad (1)$$

The spatial system is defined by the stiffness matrix \mathbf{K} and the mass matrix \mathbf{M} , both of dimension $n \times n$. \mathbf{D} is the viscous damping matrix ($n \times n$), $\mathbf{y}(t)$ the vector of outputs containing the displacements (with its derivatives in time $\dot{\mathbf{y}}(t)$ and $\ddot{\mathbf{y}}(t)$), and $\mathbf{f}(t)$ represents the vector of forces/inputs. The solution of the forward problem that determines the responses based on its excitation leads in the frequency domain to

$$\mathbf{Y}(j\omega) = \mathbf{H}(j\omega) \cdot \mathbf{F}(j\omega) \quad (2)$$

with ω as the angular frequency and $\mathbf{Y}(j\omega)$ as Fourier transform of the displacement response vector. $\mathbf{F}(j\omega)$ is the Fourier transform of the forces and $\mathbf{H}(j\omega)$ represents the $n \times n$ frequency response function (FRF) matrix. The FRF matrix $\mathbf{H}(j\omega)$ defines the dynamic characteristics of the system.

To solve the inverse problem, equation (2) needs to be inverted so that

$$\mathbf{F}(j\omega) = \mathbf{H}^{-1}(j\omega) \cdot \mathbf{Y}(j\omega). \quad (3)$$

As can be seen, an inversion of the FRF matrix is required. Equation (3) represents a determined system, in which the number of known responses equals to the number of unknown forces. So, the FRF matrix is square. As long as it is also nonsingular, equation (3) has a unique solution. However, it has to be taken into account that the inverse solution usually is ill-conditioned in the vicinity of the system resonances.

In many practical cases, it is desirable to consider a different number of known responses n than unknown forces m . Choosing $n > m$ leads to an over-determined system that enables the elimination of random errors by applying e.g., a least squares approach. A solution can be obtained in terms of the pseudo-inverse $\mathbf{H}^+(j\omega)$ (Ref. 16 and 8). The equation to solve the inverse problem results in

$$\tilde{\mathbf{F}}_{m,1}(j\omega) = \mathbf{H}_{m,n}^+(j\omega) \cdot \mathbf{Y}_{n,1}(j\omega) \quad (4)$$

where $\tilde{\mathbf{F}}(j\omega)$ represents an approximate of $\mathbf{F}(j\omega)$. The pseudo-inverse, needed in equation (4), is calculated according to

$$\mathbf{H}_{m,n}^+ = \left[\mathbf{H}_{m,n}^T \cdot \mathbf{H}_{n,m} \right]^{-1} \cdot \mathbf{H}_{m,n}^T \quad (5)$$

whereas superscript T denotes the Hermetian transpose (the transpose of the complex conjugate) of the FRF matrix \mathbf{H} .

Equations (1) to (5) are given in spatial coordinates. Usually, the system properties are known in a modal representation, such as when they are derived from system identification. Ref. 17 describes the identification of a 5-MW onshore wind turbine with a jacket foundation structure. To connect the spatial to the modal coordinates, the scaled modal matrix \mathbf{U}_0 is required. \mathbf{U}_0 results from an eigenvalue analysis of the undamped system, which is described by the stiffness and the mass matrix given in equation (1). The modal matrix consists of the eigenvectors of the system. Considering a FRF matrix in modal coordinates denoted as $\mathbf{H}_g(j\omega)$, the relation between the modal and the spatial domain is given by

$$\mathbf{H}^{-1}(j\omega) = \left(\mathbf{U}_0^{-1} \right)^T \cdot \mathbf{H}_g^{-1}(j\omega) \cdot \mathbf{U}_0^{-1}. \quad (6)$$

Finally, the inversely calculated load can be transformed into the time domain using the inverse Fourier transform applied to the vector of forces.

$$\mathbf{f}(t) = \left\{ \mathbf{F}(j\omega) \right\}^{-1} \quad (7)$$

III. Structure, load cases and simulation

To run the time-domain simulations needed to verify the inverse procedure, the comprehensive aeroelastic code FAST is used. FAST uses a nonlinear combined modal and rigid multibody formulation for modeling the dynamics of two- or three-bladed horizontal-axis wind turbines¹³. For this verification study, the NREL 5-MW reference wind turbine model is used, which is a three-bladed, upwind, horizontal-axis model, with a tubular steel tower and rigid

foundation. The turbine has a hub height of 90 m and rotor-blade lengths of 63 m. The structure is described in Ref. 18 in detail. Within the simulation, 16 degrees of freedom (DOFs) are enabled, so that the dynamics of the following components are represented: First and second flapwise blade modes (6 DOFs), 1st edgewise blade modes (3 DOFs), drivetrain rotational-flexibility (1 DOF), generator (1 DOF), yaw compliance (1 DOF), 1st and 2nd tower bending modes in fore-aft and side-side direction (4 DOFs).

To focus on the aeroelastic interaction and turbine control influences, a simple structure is desired. For that reason the tubular tower structure with a rigid foundation is chosen.

In terms of turbine control, the full-span collective blade-pitch control and variable-speed generator-torque control are enabled. FAST also provides nacelle yaw control, which is not used in this study because the influence of a changing yaw angle is not of high interest in the verification of the inverse load calculation. Only an additional coordinate transformation would be required.

Table 1: Load cases

Load case No.	Mean wind speed at hub height	Turbulence type	Turbulence characteristic
1	7 m/s	NTM ¹⁾	B ²⁾
2	12 m/s		
3	18 m/s		
¹⁾ normal turbulence model ²⁰			
²⁾ medium turbulence characteristic – 14 % turbulence intensity at 15 m/s ²⁰			

Using TurbSim¹⁹, stochastic turbulent wind fields are generated as input for the simulations. Load cases defined in IEC 61400-1 Ed. 3: 2005²⁰ under normal wind conditions for power production are chosen. Such load conditions are dominant contributions of fatigue, which the inverse load calculation aims to predict. An overview of the load cases (LCs) is given in Table 1. All of the load cases represent mean wind speeds at hub height between cut-in and rated wind speed (middle of region 2), near rated wind speed and between rated and cut-out wind speed (middle of region 3). Thus, conditions in which there are few expected control activities (load case 1) and high expected control activities (load case 3) are generated. In addition, load case 2 represents the transition between controllers where maximum thrust occurs.

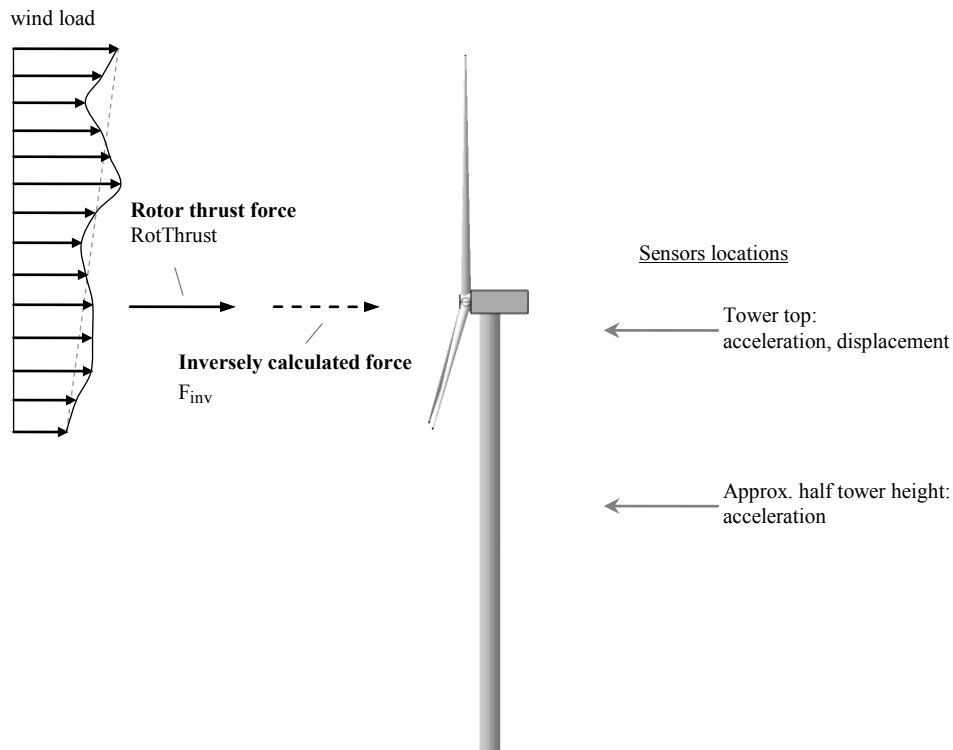


Figure 1. FAST simulation output parameter

The FAST simulations are run in a way that they correspond as closely as possible to practical field test conditions. The simulation time is set to 600 s, to match requirements from the IEC design process. Also, the time-

to frequency-domain transforms are sufficiently accurate for this simulation length. Output parameters of the wind motion and the turbine control are used for plausibility checks. Through an additional simulation – a linearization – the system matrices can be computed. The linearization simulation in FAST linearizes the nonlinear equation of motion about a given operating point and outputs the system matrices of the full system. For the inverse calculation, the system matrices are reduced to the fore-aft tower bending modes via a dynamic reduction method. Getting measurement data for the rotating blades is much more complicated than measuring the motions of fixed parts, such as the tower. Moreover, structural information of the blades is oftentimes confidential and consequently cannot be considered known data.

Parameters used in the inverse calculation are depicted in Fig. 1. The system responses at the tower top (maximum amplitude of first tower bending mode) and near half tower height (maximum amplitude of second tower bending mode) are needed. At both locations, acceleration time series are used to calculate the dynamic part of the load inversely. Although FAST also calculates tower displacements, accelerations are used because field tests usually use accelerometers to record structural motions.

In terms of the inverse load calculation, the acceleration time series are double-integrated to obtain the displacements. The integration is done using a frequency-domain approach²¹. For the double-integration, the frequency spectra need to be divided by $-(2\pi f)^2$, which has the advantage that only one calculation step is needed. This approach causes a mathematical singularity around $\omega = 0$, which is eliminated by applying a high-pass filter to the obtained displacements. With the displacements, the dynamic component can be calculated using equation (4), which is depicted in Fig. 2 by the dark grey box. In addition, displacements at the tower top in combination with known stiffness properties from the stiffness matrix \mathbf{K} are used to calculate a static/quasi-static component (light grey box in Fig. 2). To ensure compatibility to the dynamic component, the tower top displacement is low-pass filtered, so that the mean value and the low-frequency content remains. This approach is chosen due to the load characteristics with respect to the requirements of the inverse load calculation procedure and the numerical integration of the signals. The described components are superimposed to obtain the inverse load (Fig. 2). To distinguish between the quasi-static and the dynamic components, a cut-off frequency has to be chosen. This frequency is chosen at a spectral gap, so that neither exciting frequencies nor eigenfrequencies are influenced. In this study, the cut-off frequency is chosen to be 0.15 Hz.

The result of the inverse load calculation is an equivalent rotor thrust force. For verification purposes, this force will be compared to the rotor thrust force known from the FAST simulation (see Fig. 1). The rotor thrust output from FAST does not represent the applied aerodynamic thrust, but the force transmitted between the rotor and the low-speed shaft. This force includes both the applied aerodynamic thrust as well as the rotor inertia forces from the turbine vibration.

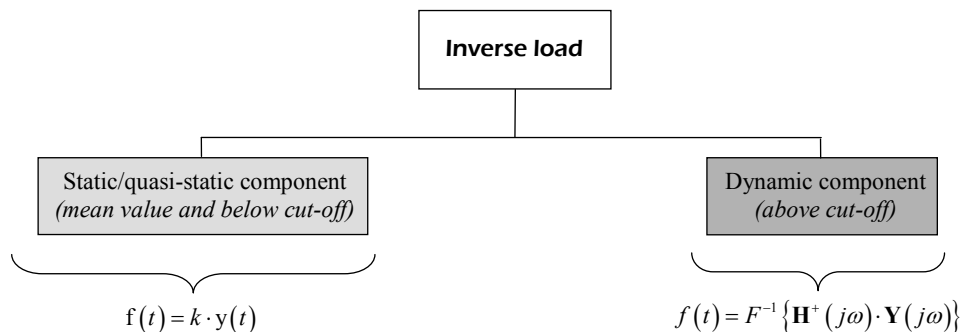


Figure 2. Overview of superposition of the components

IV. Results

The inverse calculation uses the over-determined approach, such as mentioned in equation (4). The limiting factors for the system of equations are the number of vibration modes of the system and the unknown forces that are intended to be calculated inversely. The chosen approach exclusively uses vibration modes of the support structure, which are the tower bending modes of the used model. Only the fore-aft direction is assumed to be loaded significantly of which the first and second fore-aft tower bending modes are available. Because the number of response signals must not exceed the number of vibration modes, a maximum of two response signals can be used. This study examines the inverse calculation of the applied loads for an onshore wind turbine. These loads are

dominantly caused by the instantaneous wind field at the swept rotor area. A reasonable simplification is the description of the wind loads by the rotor thrust. Therefore, the goal of the inverse load calculation of an onshore wind turbine is to determine the rotor thrust force. According to equation (4), the system of equations appears in the following form.

$$\tilde{\mathbf{F}}_{1,1}(j\omega) = \mathbf{H}_{1,2}^+(j\omega) \cdot \mathbf{Y}_{2,1}(j\omega) \quad (8)$$

The two acceleration responses are measured at the locations depicted in Fig. 1. The acceleration time series are double-integrated to obtain the displacements. In this way, the response vector $\mathbf{Y}(j\omega)$ is obtained.

The properties of the system dynamics are gained by a linearization. During linearization, FAST extracts linearized representations of the complete nonlinear aeroelastic wind turbine. This capability allows for developing the system matrices and the full-system mode shapes. The eigenvalue analysis of the system matrices gives the eigenfrequencies of the fore-aft tower bending modes as $f_{01} = 0.32$ Hz (first mode) and $f_{02} = 2.92$ Hz (second mode). Additionally, the modal matrix \mathbf{U}_0 that contains the eigenvectors column-wise is known.

To reduce the system to the fore-aft tower bending modes, a modal reduction is used. The modal reduction is based on the multiplication of the mass matrix and the stiffness matrix with a transformation matrix²². The transformation matrix contains the eigenvectors of the vibration modes that shall remain in the reduced system – in this case the eigenvectors of the fore-aft tower bending modes. The reduced system has the same eigenfrequencies as the full system. The reduced stiffness matrix \mathbf{K}_g^{red} and mass matrix \mathbf{M}_g^{red} in modal space are:

$$\mathbf{K}_g^{red} = \begin{bmatrix} 1.06 \cdot 10^6 & 0 \\ 0 & 0.92 \cdot 10^6 \end{bmatrix} \quad \text{in } Nm^{-1} \quad (9)$$

$$\mathbf{M}_g^{red} = \begin{bmatrix} 2.56 \cdot 10^5 & 0 \\ 0 & 2.73 \cdot 10^3 \end{bmatrix} \quad \text{in } kg. \quad (10)$$

The damping is assumed to be viscous modal damping. The linearization gives damping ratios that are $D_1 = 0.04$ and $D_2 = 0.01$, which enables the determination of the damping matrix \mathbf{B}_E .

$$\mathbf{B}_E = \text{diag}(2 \cdot m_{gi} \cdot \omega_{0i} \cdot D_i) \quad (11)$$

For the calculation of \mathbf{B}_E , the modal damping ratios D_i , the entries of the reduced mass matrix m_{gi} , and the eigenfrequencies $\omega_{0i} = 2\pi f_{0i}$ are needed, with i being the number of the vibration mode. Having the system description in modal space, the inverse FRF matrix in modal space can be calculated²³.

$$\mathbf{H}_g^{-1}(j\omega) = -\omega^2 \mathbf{M}_g^{red} + j\omega \mathbf{B}_E + \mathbf{K}_g^{red} \quad (12)$$

Using equation (6), the FRF matrix can be transformed back to the spatial domain. The FRF matrix still is a square matrix, since the system matrices of the reduced system are square as well. Truncating the last column of \mathbf{H} leads to the dimension (2×1) . That means, the first mode and coupling between the first and the second mode are present. Now, the pseudo-inverse is calculated according to equation (5), which allows for the solution of equation (8). In this way, the inverse load is calculated in the frequency domain. Applying equation (7) gives the time-domain representation.

A comparison of the inversely calculated force (F_{inv}) and the rotor thrust force from FAST (RotThrust) serves for the verification of the accuracy of the inverse calculation.

For each load case, the control activities that occur during the simulation are described briefly. Additionally, the inversely calculated force is compared graphically to the rotor thrust that serves as the reference value. To estimate the similarity between both forces, the quasi-static and the dynamic components are compared separately, each in the time domain and frequency domain.

A. Load case 1

Load case 1 (see Table 1) represents a mean wind speed at hub height between cut-in and rated wind speed. Load case 1 is chosen because little control activity is expected, since the variable-speed controller operates in region 2. The FAST output channels that contain the main external conditions and control activities during the simulation give the following information. The mean wind speed at hub height is about 7 m/s, which indeed represents the middle of region 2. The nacelle yaw holds a constant position. The blade-pitch angle is constant at zero, which means the three blades do not show blade-pitch control activity. The generator-torque is proportional to the square of the rotor speed in the active region.

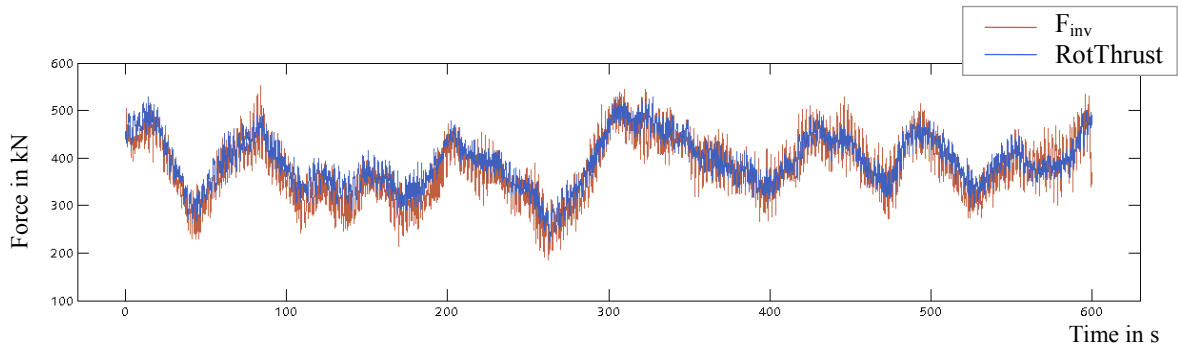


Figure 3: Rotor thrust and inversely calculated force – LC 1

Figure 3 shows the inversely calculated load compared to the rotor thrust force that is computed by FAST. The inversely calculated force follows the simulated force qualitatively.

Figure 4 gives a comparison of the quasi-static force components in the time domain and the frequency domain. Again, a very good agreement can be stated. To gain a better insight of the pure dynamic force component, Fig. 5 shows a comparison of these components in the time domain and the frequency domain. As is shown in the time domain, the inverse calculation has higher amplitudes than the simulation. Comparing the frequency spectra reveals that the differences are mainly related to the amplitudes. The frequencies of the FAST rotor thrust force also appear in the inversely calculated force, which leads to qualitatively similar frequency spectra. This observed increase amplitude of the high frequency content in the inverse load will lead to an overestimation of fatigue damage.

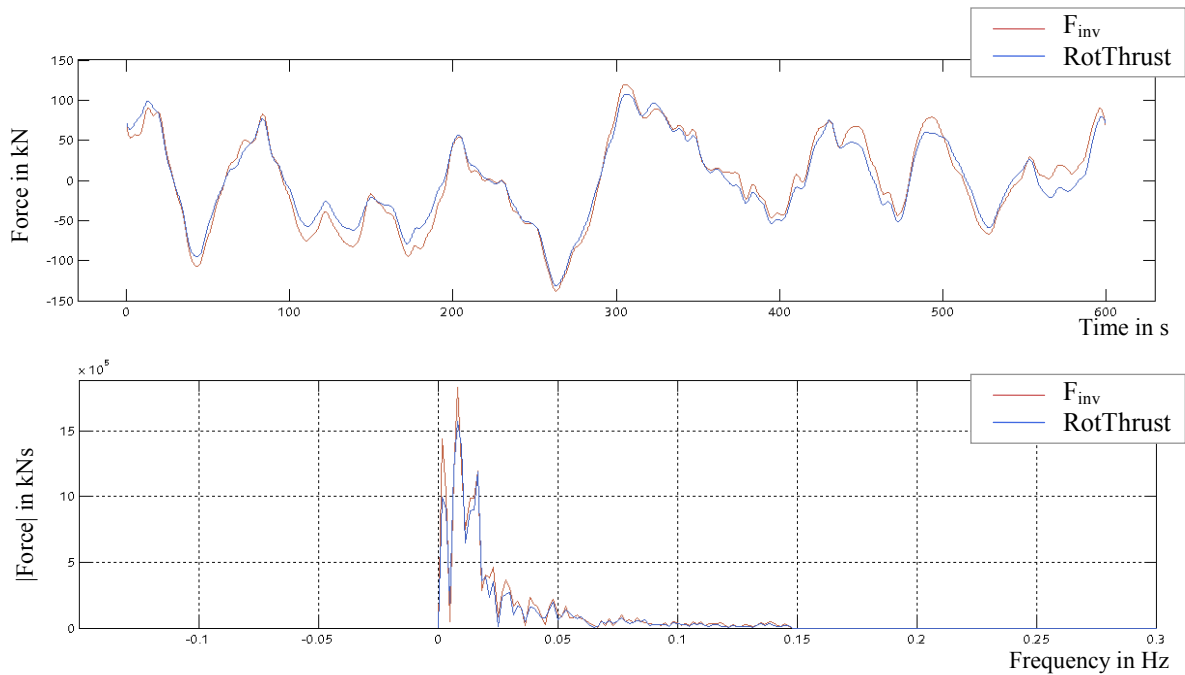


Figure 4. Quasi-static components – LC 1

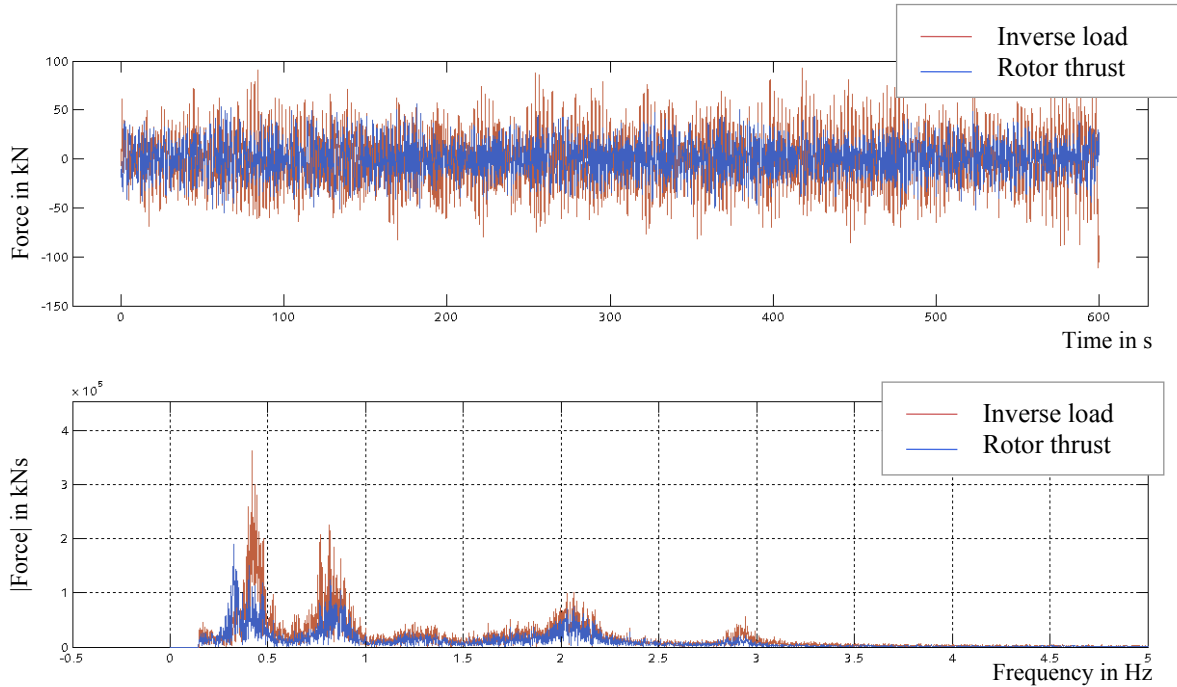


Figure 5: Dynamic components – LC 1

B. Load case 2

Load case 2 (see Table 1) represents a mean wind speed at hub height near rated wind speed. This load case represents the transition between controllers, where maximum thrust occurs. The mean wind speed at hub height is approximately 12 m/s, which is near rated wind speed. The generator torque is no longer proportional to the rotor speed. Again, the nacelle yaw position is constant around zero. Now, blade-pitch control shows activity during the simulation. Since collective blade-pitch control is enabled, all three blades follow exactly the same control algorithm. The blade pitch angle varies between 0° and 10° .

Figure 6 shows the result of the inverse calculation. As were found in load case 1, the inversely calculated load and the rotor thrust are compared. Again, a good match between both signals is visible.

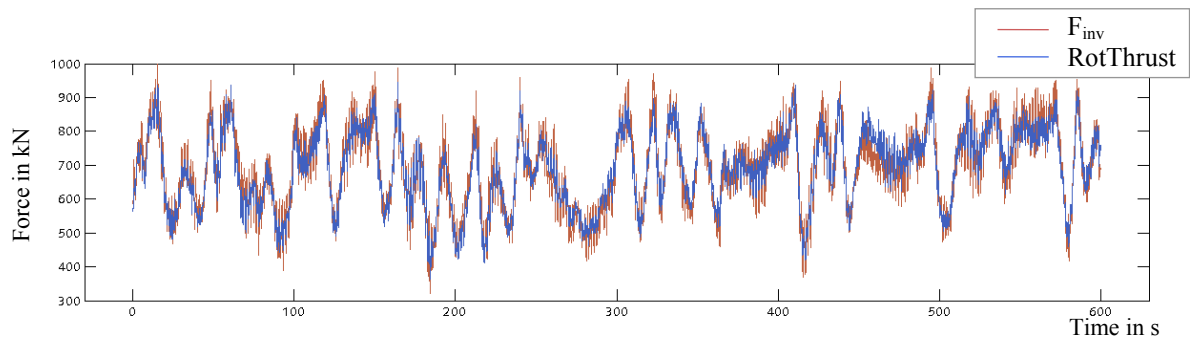


Figure 6: Rotor thrust and inversely calculated force – LC 2

The quasi-static components are depicted in Fig. 7, both in the time domain and frequency domain. Both graphs match nearly perfect. An analog depiction is given in Fig. 8 for the dynamic components. The comparison of the dynamic components in the time domain and the frequency domain leads to similar results as gained for LC 1. The inverse calculation shows higher amplitudes than the reference rotor thrust in the time-domain comparison. Indeed, the characteristics of the frequency spectrum are calculated well by the inverse procedure. The peaks of the rotor thrust are very similar, but the amplitude of the inversely calculated rotor thrust is higher than the amplitude of the rotor thrust from FAST.

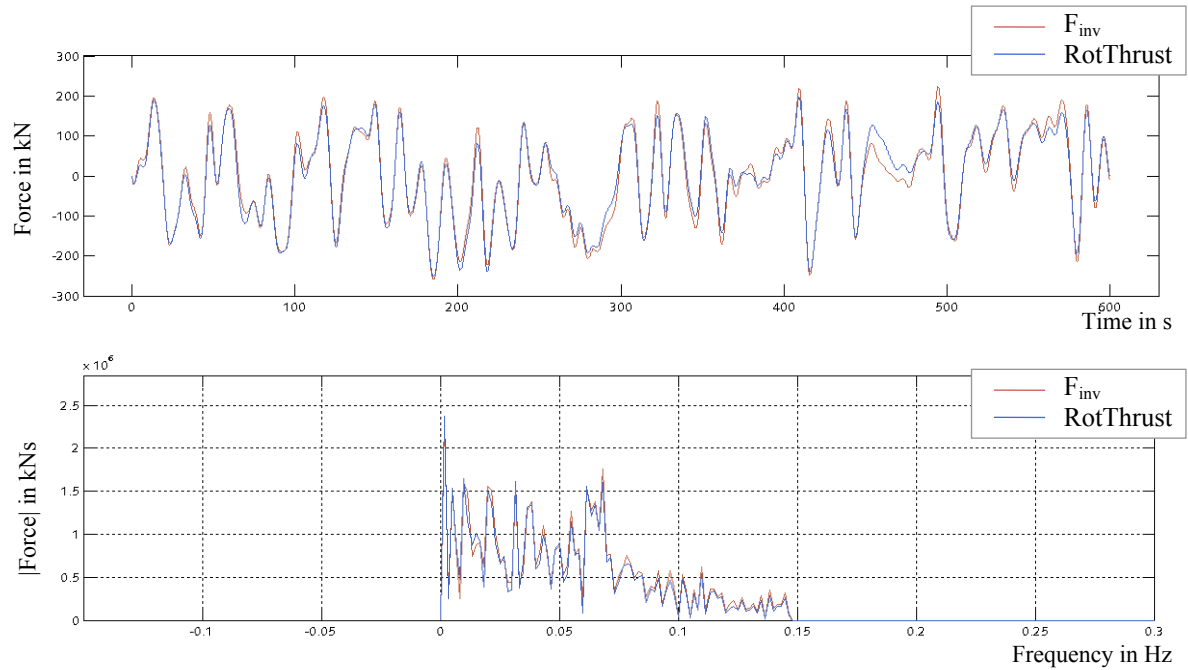


Figure 7. Quasi-static components – LC 2

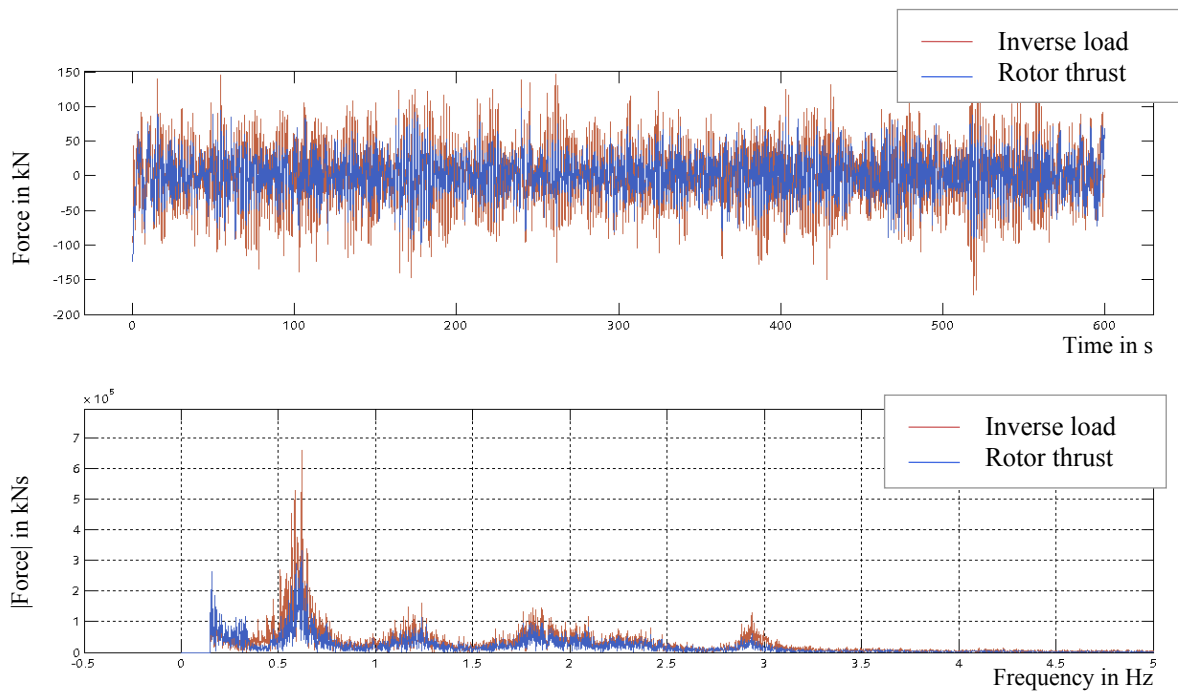


Figure 8. Dynamic components – LC 2

C. Load case 3

Load case 3 (see Table 1) represents a mean wind speed at hub height between the rated and cut-out wind speeds (middle of region 3). Load case 3 is chosen because high control activity is expected. The main external conditions and control activities of this load case are the following. The mean wind speed at hub height is at 18 m/s, which indicates the middle of region 3. As for load cases 1 and 3, the yaw position is constant at zero. The collective blade-

pitch angle ranges between 10° to 20° . While the torque controller operates in region 3, relative to region 2, the control strategy has changed from “optimal power” in region 2 to “constant power” in region 3.

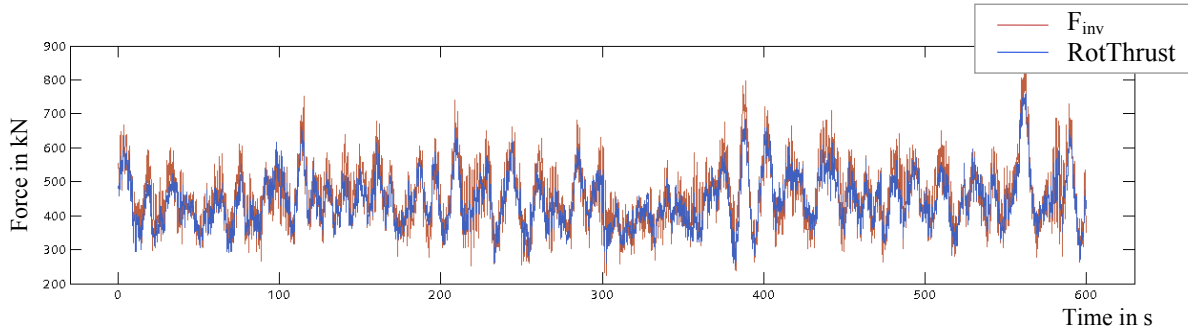


Figure 9: Rotor thrust and inversely calculated force – LC 3

An illustration of the result of the inverse load calculation for load case 3 is shown in Fig. 9. The inversely calculated load and the rotor thrust of the FAST simulation are depicted. As visible, both signals show a very good agreement, as is the case for load cases 1 and 2 as well.

The quasi-static components are depicted in Fig. 10, both in the time domain and the frequency domain. The excellent agreement of both force components is visible. Figure 11 shows the time-domain and frequency-domain depiction of the dynamic component. As already seen for the load cases 1 and 2, the inverse process calculates similar frequencies as occur for the FAST rotor thrust force. Again, the amplitudes of the inversely calculated force are higher than the amplitudes of the rotor thrust, which is true for both the time-domain and the frequency-domain comparisons.

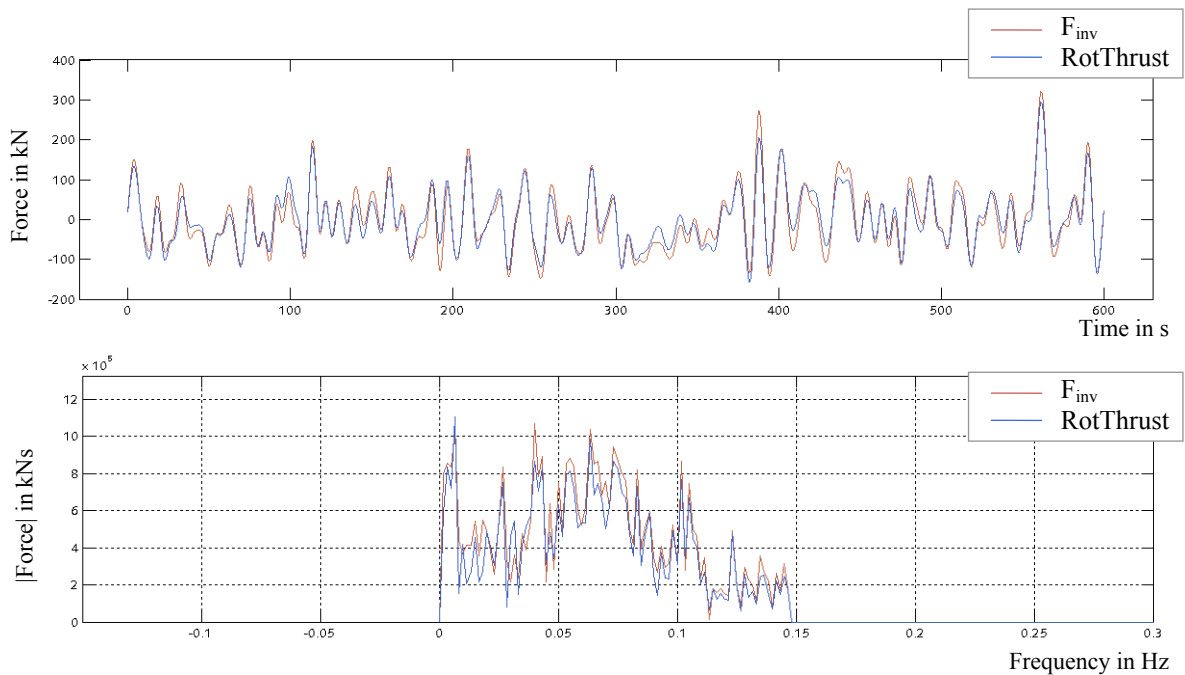


Figure 10. Quasi-static components – LC 3

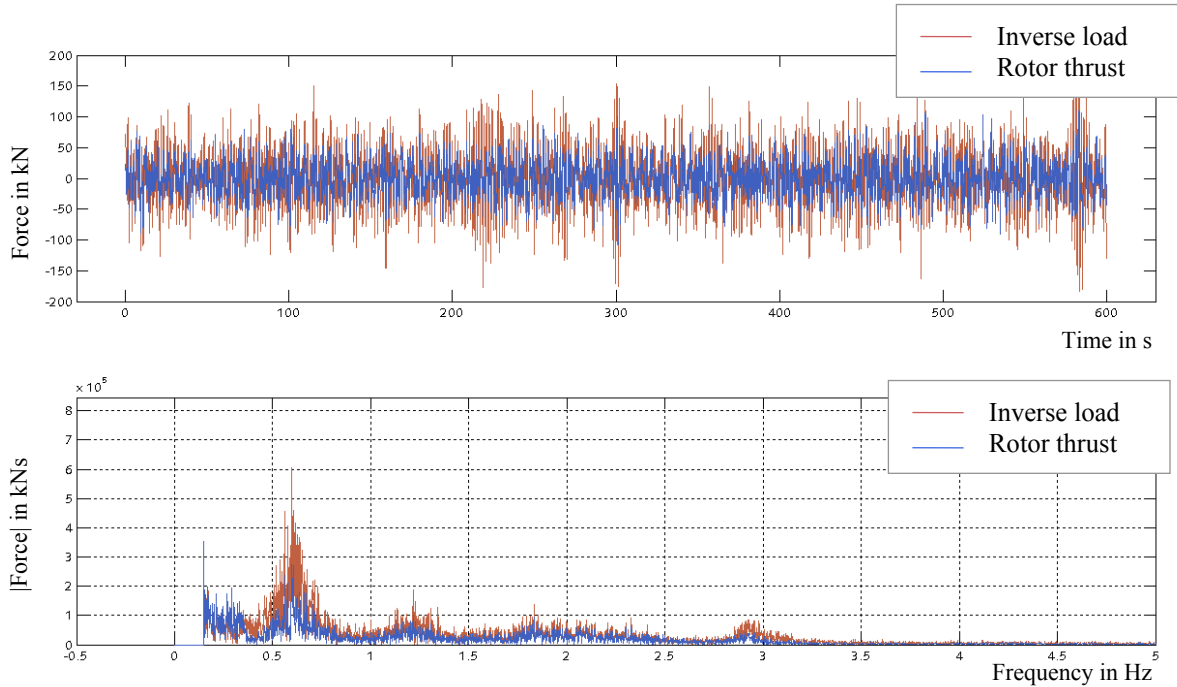


Figure 11. Dynamic components – LC 3

D. Summary of the load cases

All three load cases show similar characteristics in terms of the accuracy of the results for the inverse calculation. The static/quasi-static components are calculated with a very good agreement. The dynamic components contribute most to the observed differences between the inversely calculated force and the rotor thrust. The inversely calculated load partly has twice the amplitude. Hence, the reason for the differences is assumed to be part of the inverse calculation of the dynamic parts. The mathematics of the underlying equations produce exact results, as can be shown using simple numerical examples. But, the inverse calculation is based on an important assumption. The system used for the inverse calculation is a reduced system. The reasons for the reduction are described in section III. So, the rotor thrust force is derived using the full system description, whereas the inverse load is calculated with a reduced system. The reduction only affects the inverse calculation of the dynamic components where the main contribution to the differences occur. Thus, the system reduction is assumed to be the main reason for the observed differences. Because the differences are considered acceptable, the system reduction is an appropriate assumption. As indicated by the results of the three presented load cases, the inverse calculation tends to produce force amplitudes that are always slightly higher than the amplitudes of the reference force.

The resulting quality of the inverse load calculation is similar for the three load cases. Consequently, the inverse calculation does not depend on the control activities of the wind turbine. The three load cases were set up to represent different operating conditions with different control activities. Because the differences do not vary significantly, the stated conclusion is demonstrated.

V. Conclusion and Outlook

This paper presents a numerical verification study of an inverse load calculation procedure. The inverse load calculation is done for a 5-MW onshore wind turbine structure using a model of the system dynamics and system responses, both simulated with the comprehensive simulation code FAST. This approach accounts for coupled dynamics and turbine control. For verification, the inversely calculated load is compared to the known rotor thrust from the FAST simulation. A concept for superimposing the inverse load by a static/quasi-static component and a dynamic component is demonstrated. The theoretical bases of the dynamic inverse load calculation are discussed.

As shown, the inverse load calculation is capable of generating good estimates of the applied load, which is shown for simulations that account for coupled dynamics of wind inflow, aerodynamics, elasticity and turbine control.

Three different load cases are simulated. The load cases are set up so that little control activity, maximum rotor thrust, and high control activity occur. The results show that the accuracy of the inverse load calculation does not depend on the control activity of the wind turbine.

The presented study shows the ability of the inverse load calculation to derive the applied loads for onshore wind turbines, represented by the rotor thrust. In practice, the rotor thrust can be measured. Consequently, the application of the inverse load calculation is useful if the measurement of the rotor thrust is impeded e.g., by prohibited/hindered accessibility. Another potential application for the inverse load calculation would be for systems with more complicated load conditions, such as those caused by combined wind and wave loads.

For that reason, further studies will investigate the capability of the inverse load calculation to compute combined wind and wave loads for an offshore wind turbine. Again, a numerical study that uses the comprehensive simulation code FAST will be performed.

Eventually, the inverse load calculation is intended to be used for lifetime predictions using measurement data of offshore wind turbines. The fatigue-strength analysis mainly depends on the range of stresses. Assuming a linear dependency between the loads and the stresses, as is done for steel under normal operational conditions, the quasi-static and the dynamic component of the inverse load will be used for the fatigue analysis. The quasi-static component shows an excellent agreement and the dynamic component contains amplified amplitudes. Consequently, using inversely calculated loads for fatigue analysis is a safe assumption. This conclusion is also valid in case of nonlinear load-to-stress relations, as occurs for reinforced concrete. Then, the mean values of the stresses have to be taken into account additionally, which depends on the static component that shows an excellent accuracy as well.

Acknowledgments

The presented research was done during a scientific research exchange of T. Pahn at the National Renewable Energy Laboratory (NREL) in Golden CO, USA. T. Pahn cordially thanks the NREL staff for their remarkable support. T. Pahn also thanks the German Academic Exchange Service that funded the scientific exchange.

References

- ¹IEC Technical Standard 61400-13, "Wind Turbine Generator Systems – Part 13: Measurement of mechanical loads," First Edition 2001-06, International Electrotechnical Commission, Geneva Switzerland, 2001.
- ²Federal Maritime and Hydrographic Agency, *Standard – Design of Offshore Wind Turbines*, BSH-No. 7005, Hamburg and Rostock, Germany, 2007, URL: <http://www.bsh.de/en/Products/Books/Standard/7005eng.pdf> [cited 08 February 2012].
- ³Williams, D., Jones, R. P. N., "Dynamic Loads in Aeroplanes under given Impulsive Loads with Particular Reference to Landing and Gust Loads on a large Flying Boat," Aeronautical Research Council Tech Report No. 2221, 1948.
- ⁴Bartlett, F. D. Jr., Flanelli, W. G., "Model Verification of Force Determination for Measuring Vibratory Loads," *Journal of the American Helicopter Society*, Vol. 24, April 1979, pp. 10-18.
- ⁵Nordberg, Patrik L., "Time-domain Methods for Load Identification of Linear and Nonlinear Systems," Ph.D. Dissertation. Chalmers University of Technology. Department of Applied Mechanics, Göteborg, Sweden, 2004, ISBN 91-7291-489-0.
- ⁶Nordström, Lars J. L., "Input Estimation in Structural Dynamics," Ph.D. Dissertation, Chalmers University of Technology. Department of Applied Mechanics, Göteborg, Sweden, 2005, ISBN 91-7291-668-0.
- ⁷Romppanen, A.-J., "Inverse Load Sensing Method for Line load Determination of Beam-Like Structures," Ph.D. Dissertation, Tampere University of Technology, Finland, 2008, ISBN 987-952-15-2053-2.
- ⁸Menke, W., *Geophysical Data Analysis: Discrete Inverse Theory*, Academic Press Inc., San Diego, USA, 1984, ISBN 0-12-490921-3.
- ⁹Fritzen, C.-P., Klinkov, M., "Online Wind Load Estimation for Offshore Wind Energy Plants," *Proceedings of the 6th International Workshop on Structural Health Monitoring*, edited by F.-K. Chang, Stanford, CA, USA, Sept. 2007, pp. 1905-1912.
- ¹⁰Swartz, R. A., Zimmermann, A. T., Lynch, J. P., "Automated Wind Load Characterization of Wind Turbine Structures by Embedded Model Updating," *Proceedings SPIE 7647*, 76470J, 2010; doi:10.1117/12.847697.
- ¹¹Abschlussbericht zum Forschungs- und Entwicklungsprojekt IMO-Wind, „Integrales Monitoring- und Bewertungssystem für Offshore-Windenergieanlagen, Teil: Methoden zur Datenanalyse und Schadensfrüherkennung,“ Projekt-Nr. 16INO326, edited by W. Rücker and C.-P. Fritzen, Berlin, Germany, 2010.
- ¹²Pahn, T, Rolfes, R, „Inverse Belastungsermittlung, Kapitel 6.5 des Abschlussberichtes zum Verbundprojekt OGOWin - Optimierung aufgelöster Gründungsstrukturen für Offshore Windenergieanlagen,“ pp. 274-280, edited by WeserWind GmbH Offshore Construction, Bremerhaven, Germany, 2010.
- ¹³Jonkman, Jason; Buhl, Marshall: *FAST User's Guide*. Technical Report NREL/EL-500-38230, August 2008, URL: <http://wind.nrel.gov/designcodes/simulators/fast/> [cited 08 February 2012].
- ¹⁴Klinkov, M., Fritzen, C.-P., "An Updated Comparison of the Force Reconstruction Methods," *Key Engineering Materials*, Vol. 347, 2007, pp 461-466.

¹⁵Pahn, T, Rolfes, R, “OGOWin – Optimization of Jacket Foundation Structures for Offshore Wind Turbines Concerning Material Consumption, Assembling Order and Manufacturing Process,” Annual ForWind Report 2009, pp. 54-55, URL: www.forwind.de [cited 08 February 2012].

¹⁶Stevens, K., “Force Identification Problems – an overview,” *Proceedings of SEM*, Spring Meeting 1987, pp. 838-844.

¹⁷Pahn, T., Rolfes, R, Kohlmeier, M., “System identification of a jacket support structure for a 5 MW offshore wind turbine due to artificial and ambient excitation,” *Proceedings of Torque*, edited by S. Voutsinas, Athens, June 2010 , pp 769-780.

¹⁸Jonkman, J., Butterfield, W., Musial, W., Scott, G., *Definition of a 5-MW Reference Wind Turbine for Offshore System Development*, Technical Report NREL/EL-500-38060, February 2009, URL: <https://ceprofs.civil.tamu.edu/jzhang/ocen407/5MW%20Reference%20Turbine.pdf> [cited 08 February 2012].

¹⁹Jonkman, B. J., *TurbSim User's Guide- TurbSim version 1.50*, Technical Report NREL/TP-500-46198, Sept. 2009, URL: <http://wind.nrel.gov/designcodes/preprocessors/turbsim/TurbSim.pdf> [cited 08 February 2012].

²⁰IEC Technical Standard 61400-1, “Wind turbines – Part 1: Design requirements,” Third Edition, International Electrotechnical Commission, Geneva Switzerland, 2005.

²¹Mercer, C. , *Acceleration, Velocity and Displacement Spectra – Omega Arithmetic*, Prosig Signal Processing Tutorials, 2006, URL: <http://blog.prosig.com/2006/12/07/acceleration-velocity-displacement-spectra-%E2%80%93-omega-arithmetic/> [cited 08 February 2012].

²²Gasch, R., Knothe, K., *Strukturdynamik – Band 2: Kontinua und ihre Diskretisierung*. Springer Verlag, Berlin Heidelberg, 1989, ISBN 3-540-50771-X.

²³Ewins, D. J., *Modal Testing – theory, practice and application*, Second edition, Research Study Press Ltd. Baldock, England, 2000, ISBN 978-0-86380-218-8.